Title

Temperature effects in plasma-based positron acceleration schemes using electron filaments

Journal

Physics of Plasmas, 30(7)

ISSN

1070-664X

Authors

Diederichs, S
Benedetti, C
Esarey, E
et al.

Publication Date

2023-07-01

DOI

10.1063/5.0155489

Peer reviewed

Temperature effects in plasma-based positron acceleration schemes using electron filaments

S. Diederichs,[1, 2, 3, a)] C. Benedetti,[2] E. Esarey,[2] M. Thévenet,[1] A. Sinn,[1] J. Osterhoff,[1] and C. B. Schroeder[2, 4]
[1)] *Deutsches Elektronen-Synchrotron DESY, Notkestr. 85, 22607 Hamburg, Germany*
[2)] *Lawrence Berkeley National Laboratory, Berkeley, California 94720, USA*
[3)] *University of Hamburg, Institute of Experimental Physics, Luruper Chaussee 149, 22607 Hamburg, Germany*
[4)] *Department of Nuclear Engineering, University of California, Berkeley, California 94720, USA*

(Dated: 18 July 2023)

Preserving the quality of a positron beam in a plasma-based accelerator where a wakefield suitable for positron transport and acceleration is generated by means of an electron filament is challenging. This is due to the nature of the wakefields, characterized by focusing fields that vary nonlinearly in the transverse direction, and accelerating field that are non-uniform. These fields also change slice-by-slice along the beam. Maintaining a high beam quality is pivotal for application of positron beams in a plasma-based collider. In this paper we show that an initial background plasma temperature can help mitigate the positron beam quality degradation in plasma-based accelerators that rely on electron filaments. We show that temperature effects broaden the electron filament and smooth radially both the non-linear transverse and the non-uniform longitudinal wakefields. Using warm plasmas opens up new possibilities to improve beam quality in several plasma-based positron acceleration concepts.

I. INTRODUCTION

Plasma-based accelerators are promising candidates as drivers for a future linear electron-positron collider, due to the large accelerating fields they can produce. For a linear collider, high beam quality is crucial to achieve a sufficient luminosity. While high-quality electron acceleration has been demonstrated in plasma accelerators using the so-called blowout regime[1,2], the acceleration of high-quality positron bunches is more challenging owing to the asymmetric plasma response[3–6]. To generate fields within a plasma that are both accelerating and focusing for positrons, an area of high electron density is needed. Due to the high mobility of the plasma electrons, these areas of high electron density usually feature slice-dependent, transversely non-linear focusing and non-uniform accelerating wakefields, which can degrade the positron beam quality. In this work, we show that the beam quality degradation is mitigated by a plasma temperature.

Various schemes have been proposed to generate the high-density electron filaments required for positron acceleration, e.g., using plasma columns[7–9], utilizing the posterior region of a blowout wake[10–13], employing quasi-hollow plasma channels[14], or hollow core plasma channels operating in the nonlinear regime[15]. Most of these schemes use plasma targets that are either generated by optical field ionization (such as plasma columns[16–18] or hollow core plasma channels[19]), or homogeneous plasmas that are generated by electrical discharges. In both methods the plasma electrons can have a temperature of a few to tens of eV[17,20,21]. In general, a plasma temperature is known to reduce the wave-breaking field amplitude[22–25]. In the blowout regime, temperature effects were found to reduce the spike of the longitudinal wakefield at the back of the bubble[26,27]. This reduction in the electron density spike amplitude did not affect the energy gain or energy spread of the accelerated electron beams[27] since the spike at the back of the bubble itself cannot be used for electron acceleration. Owing to the lack of impact in the context of electron acceleration, plasma temperature is often neglected when modeling plasma wakefield accelerators (i.e., the background plasma is modeled as cold). However, as discussed in this work, for most plasma-based positron acceleration schemes the influence of an initial background plasma temperature is found to be significant.

The importance of temperature effects for plasma-based positron acceleration has already been identified in two positron acceleration schemes that explicitly rely on temperature to generate the positron accelerating field structure. One of the schemes utilizes the thin, warm, quasi-hollow plasma channels that arise during the long-term plasma dynamics in the aftermath of a blowout wake[14] to generate the required electron density filament. The other one uses a temperature of tens of eV and an electron witness bunch to elongate the electron density spike at the back of the blowout[13]. In the latter, the temperature was also reported to broaden the electron filament, thereby increasing the transverse extend of the linear focusing field for positron beams.

In this work, we demonstrate the crucial role of the plasma temperature in different positron acceleration schemes that rely on narrow, high-density electron filaments, which has been previously overlooked. The temperature-induced transverse broadening of the nar-

[a)] Electronic mail: severin.diederichs@desy.de.

row electron filaments leads to a transverse smoothing of the non-linear focusing and the non-uniform accelerating fields within these structures. In turn, the smoothing mitigates the beam quality degradation of accelerated positron bunches.

The article is structured as follows: In Sec. II, the implementation of a background plasma with an initial temperature in the quasi-static particle-in-cell (PIC) code HiPACE++ is discussed. In Sec. III, the effect of a plasma temperature is presented for two positron acceleration schemes that are based on high-density electron filaments, namely positron acceleration in a plasma column and positron acceleration in a hollow core plasma channel. Sec. IV concludes this work.

II. NUMERICAL IMPLEMENTATION

The implementation of a plasma temperature in a quasi-static PIC code has been discussed in Jain *et al.*[27] for the 2D (cylindrical) quasi-static PIC code WAKE[28]. Here, we briefly revisit the core idea to motivate the implementation in the 3D quasi-static, GPU-accelerated, PIC code HiPACE++[29].

A quasi-static PIC code utilizes the disparity of time scales that typically characterizes the physics in a plasma-based accelerator: ultra-relativistic beams or laser pulses evolve slowly compared to the plasma response, and can therefore be advanced with large time steps. The plasma response is calculated in the co-moving coordinate $\zeta = z - ct$, with z the longitudinal coordinate, t the time, and c the speed of light. The normalized Hamiltonian $\mathcal{H}$ for a plasma electron in the co-moving variable is given by[28,30]

$$\mathcal{H} = \sqrt{1 + |\mathbf{U} + \mathbf{a}|^2} - \phi - U_z = \gamma - \psi - u_z \,, \quad (1)$$

with the normalized canonical momentum $\mathbf{U} = \mathbf{u} - \mathbf{a}$, $\mathbf{u}$ and $\mathbf{a}$ being the normalized particle momentum and vector potential, respectively, and the pseudo-potential $\psi = \phi - a_z$.

If the quasi-static approximation is valid, the Hamiltonian is constant in time, i.e., $\mathrm{d}\mathcal{H}/\mathrm{d}t = 0$, such that $\gamma - \psi - u_z$ is a constant of motion for the plasma particles. For an initially cold and unperturbed plasma (i.e., $\psi_0 = 0$, $u_{z,0} = 0$, $\gamma_0 = 1$), the constant of motion equals 1. For a warm plasma, however, the particles have an initial thermal momentum. The constant of motion for a warm, unperturbed (i.e., $\psi_0 = 0$) plasma particle is then given by

$$\gamma - \psi - u_z = \gamma_0 - u_{z,0}, \quad (2)$$

with $\gamma_0 = \sqrt{1 + \mathbf{u}_0^2}$ being the initial Lorentz factor of the plasma particle. Thus, the constant of motion of each plasma particle depends on its thermal momentum at initialization. For a Maxwellian temperature distribution, the initial plasma particle momenta are normally distributed with a variance $k_B T/(Mc^2)$ in each dimension, with M the particle mass, k_B the Boltzmann constant, and T the isotropic temperature. For convenience, the temperature $k_B T$ is henceforth given in eV. To model a plasma temperature in a quasi-static PIC code, the plasma must be initialized with the corresponding momentum, and the correct constant of motion must be used throughout the code, e.g., in the particle pusher or current deposition (see Jain *et al.*[27] for more details). In the following studies, the ions are assumed to be cold and immobile.

We implemented the quasi-static temperature model above in HiPACE++ and benchmarked it against the fully electromagnetic 3D PIC code WarpX[31]. For the comparison, a wake in the blowout regime is considered. The test setup consists of two Gaussian electron beams, a driver and a witness beam, propagating in a uniform plasma with a density of $n_0 = 10^{16}\mathrm{cm}^{-3}$. The drive beam has a peak density of $n_d/n_0 = 10$, a transverse rms size of $\sigma_{x/y,d} = 0.3\, k_p^{-1}$, and a longitudinal rms size of $\sigma_{z,d} = 1.41\, k_p^{-1}$. The witness beam has a peak density of $n_w/n_0 = 100$, a transverse rms size of $\sigma_{x/y,w} = 0.1\, k_p^{-1}$, and a longitudinal rms size of $\sigma_{z,w} = 0.2\, k_p^{-1}$. Thereby, $k_p^{-1} = c/\omega_p$ is the plasma skin depth, which is the characteristic length scale in the plasma, and $\omega_p = \sqrt{4\pi n_0 e^2/m_e}$ the plasma frequency with e being the elementary charge and m_e the electron mass, respectively. The plasma is modelled with 1 macro-particle per cell, the beams are modelled with 1 macro-particle per cell (the spatial profile is captured by adjusting the macro-particle weights). The computational domain is $(-8, 8) \times (-8, 8) \times (-7, 5)\, k_p^{-3}$ in $x \times y \times \zeta$, where x and y are the transverse coordinates. The mesh resolution is $0.016 \times 0.016 \times 0.012\, k_p^{-3}$.

The resulting on-axis longitudinal wakefield E_z/E_0 is plotted against the co-moving variable ζ in Fig. 1 (a), (b), and (c) for a plasma temperature of 0 eV, 50 eV, and 500 eV, respectively. The electric fields are normalized to the cold, non-relativistic wave-breaking field $E_0 = m_e c^2 k_p / e$. A reasonable agreement between HiPACE++ (solid blue lines) and WarpX (dashed orange lines) is found, verifying the temperature implementation in HiPACE++.

III. TEMPERATURE EFFECTS

Having benchmarked the implementation of temperature in the quasi-static PIC code, we now investigate via simulations the temperature effects in two positron acceleration schemes that rely on high-density electron filaments: positron acceleration in a plasma column and positron acceleration in a hollow core plasma channel.

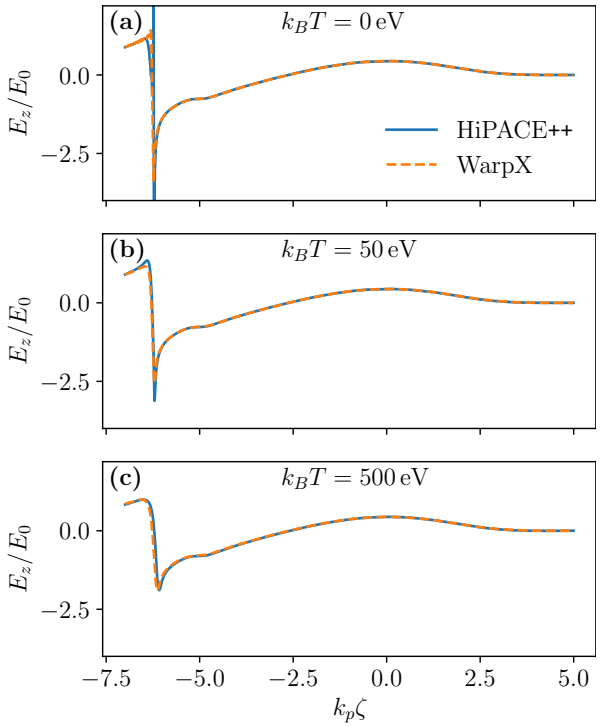

FIG. 1. On-axis longitudinal wakefield, E_z/E_0, versus co-moving variable, $k_p\zeta$, for (a) a cold plasma, (b) a plasma at 50 eV, and (c) a plasma at 500 eV. The codes show reasonable agreement for all presented temperatures.

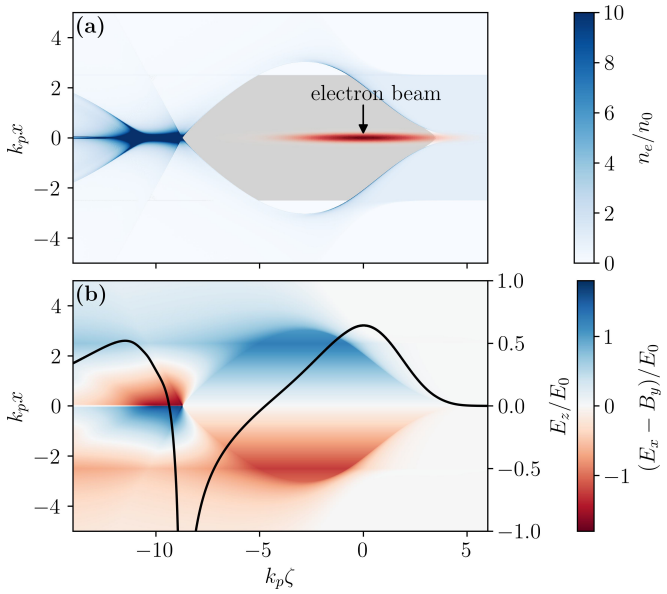

FIG. 2. Schematic of positron acceleration in a plasma column. (a) Electron drive beam (red), normalized plasma density (blue), and ion background (grey) in the x-ζ-plane. The drive beam excites a plasma wake with a blowout radius larger than the column radius, thereby generating an intense on-axis electron filament at $-14 < k_p\zeta < -9$. (b) Transverse wakefield in the x-ζ-plane (red-blue) and on-axis longitudinal wakefield (black line) along the co-moving variable ζ. The electron filament generates an accelerating and focusing field structure for positrons.

A. Positron acceleration in a plasma column

Plasma columns are a promising candidate for high-quality, stable positron acceleration[7–9,32]. In the scheme, an electron drive beam propagates along the axis of a finite-radius plasma column. When the electron beam drives a wake in the blowout regime, where the blowout radius exceeds the radius of the plasma column, the plasma electron trajectories of the electron sheath are altered due to a lack of ions outside the column. Then, the focusing force acting on the plasma sheath electrons is reduced and the electrons return back to the axis in an elongated filament at some distance behind the driver. The electron filament provides both accelerating and focusing fields for positron beams.

The following reference setup is used to demonstrate the scheme via simulations using HiPACE++. The setup consists of a Gaussian drive beam and a plasma column with a radius of $R_p = 2.5\,k_p^{-1}$. The drive beam has a peak current of $I_b/I_A = 1$, with $I_A = m_e c^3/e \approx 17\,\mathrm{kA}$ being the Alfvén current. The drive beam is modelled with 10^8 macro-particles. The plasma electrons are modelled with 49 macro-particles per cell. In the simulations, the computational domain is $(-16, 16) \times (-16, 16) \times (-14, 6)\,k_p^{-3}$ in $x \times y \times \zeta$. The mesh resolution is $0.0078 \times 0.0078 \times 0.002\,k_p^{-3}$. Note that the fields within the electron filament converge slowly, therefore, a fine resolution is needed. The scheme is illustrated in Fig. 2, where the normalized electron density is shown in the x-ζ-plane in (a). The ion background and the electron drive beam are denoted in grey and red, respectively. The resulting transverse wakefield and a lineout of the on-axis longitudinal wakefield (black line) are shown in Fig. 2 (b). The on-axis electron filament between $-14 < k_p\zeta < -10$ generates both accelerating and focusing fields for positron beams. For a cold plasma, the resulting transverse wakefield in the electron filament is close to a step-like profile along the transverse coordinate[7]. Despite being non-linear, a Gaussian witness bunch can be quasi-matched to these non-linear focusing fields to limit the emittance growth to a few percent[7].

We now investigate the effect of a temperature on the fields within the electron filament by simulations using HiPACE++. Starting from the base configuration, we scan the temperature from 10 eV to 100 eV. Lineouts of the on-axis longitudinal wakefield E_z/E_0 along the co-moving variable ζ and of the transverse wakefield $(E_x - B_y)/E_0$ along the transverse coordinate x at $\zeta = -10.5\,k_p^{-1}$ are shown in Fig. 3 (a) and (b), respectively, for different values of the temperature. The acceleration phase for positrons between $-14 < k_p\zeta < -10$ is only slightly decreased by temperatures above 50 eV. On the other hand, the transverse wakefield is significantly altered already at 10 eV. The slope of the transverse wakefield at the zero-crossing decreases with an in-

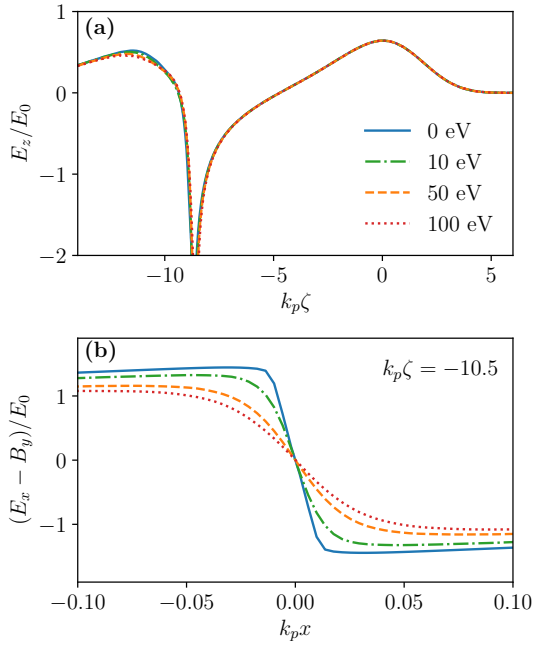

FIG. 3. (a) Longitudinal wakefield E_z/E_0 versus co-moving variable $k_p\zeta$ and (b) transverse wakefield amplitude $(E_x - B_y)/E_0$ versus transverse position k_px at $k_p\zeta = -10.5$ for various plasma temperatures. A temperature of 50 eV and above reduces the accelerating gradient only slightly. However, even small temperatures reduce the transverse wakefield amplitude and significantly broaden the region where the wakefield varies linearly with the transverse coordinate.

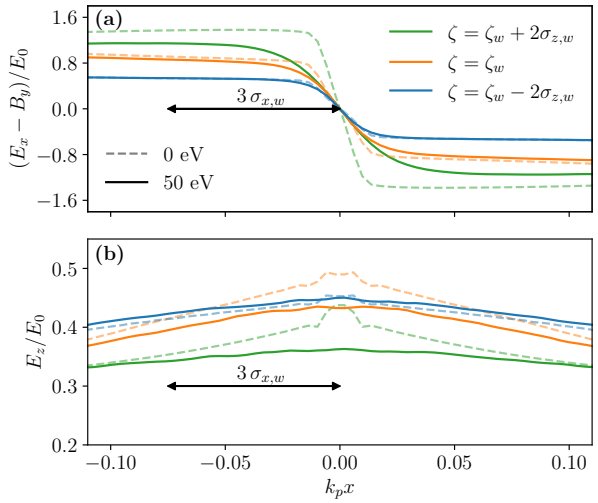

FIG. 4. Transverse (a) and longitudinal (b) wakefields along transverse coordinate k_px at tail (blue lines), center (orange lines), and head (green lines) of the witness bunch for a plasma with 0 eV (dashed lines) and 50 eV (solid lines), respectively. The smoothing of both the transverse and the longitudinal wakefield around $k_px = 0$ due to the temperature is more pronounced at the head of the beam.

creasing temperature. Furthermore, the maximum field amplitude at the sides is reduced. Overall, the non-linear transverse wakefield is smoothed by the temperature. The reason is that due to the initial thermal transverse momentum of the plasma electrons, they do not return exactly on the propagation axis of the beam, but instead only in the vicinity of the axis. Therefore, the electron filament is transversely broadened, leading to a less sharp on-axis density profile. As a consequence, the non-linear transverse wakefield is smoothed.

The broadening of the electron filament due to a temperature also has a significant effect on the numerical convergence. In a cold plasma, when all electrons return precisely on the propagation axis, the sharp density spike is difficult to resolve and the fields converge slowly. Due to the broadening of the electron filament by the temperature, the on-axis density spike can be resolved more easily and the fields converge more rapidly. In fact, a small temperature is needed to ensure convergence at a reasonable resolution. The temperature-dependent convergence is discussed in more detail in the Appendix.

We now examine the effect of the temperature on the transverse wakefield in the presence of a strong positron witness bunch. Thereby, the positron witness beam is located in $\zeta_w = -11.57\,k_p^{-1}$ and has a bi-Gaussian shape with rms sizes $\sigma_{x/y,w} = 0.025\,k_p^{-1}$ and $\sigma_{z,w} = 0.5\,k_p^{-1}$. It has a peak density of $n_w/n_0 = 500$ and an initial emittance of $\epsilon_{x/y} = 0.1\,k_p^{-1}$. The positron beam is modelled with 7.5×10^7 macro-particles. The transverse and longitudinal wakefields are shown in Fig. 4 (a) and (b), respectively, at three different longitudinal locations for a cold plasma (0 eV, dashed lines) and a warm plasma (50 eV, solid lines). Both the transverse and the longitudinal wakefields are significantly smoothed by the temperature. Notably, the smoothing effect of the temperature is particularly prominent towards the head of the beam (green lines), i.e., at phases around $\zeta_w + 2\sigma_z$. There, the amplitude of both fields is reduced in the warm plasma. The slope of the transverse wakefield around the zero-crossing is reduced and, consequently, the head-to-tail variation of the transverse wakefield is reduced. The longitudinal wakefield is more uniform around the zero-crossing at a plasma temperature of 50 eV. At the center of the beam (orange lines) and at the tail of the beam (blue lines), defined as $\zeta_w - 2\sigma_z$, the smoothing of the wakefield around the zero-crossing is still observed, but the effect is significantly smaller than at the head of the beam. The transverse beam size exceeds the smoothed area of the wakefields, as shown by the black arrow in Fig. 4, which indicates the characteristic beam width.

To study the effect of temperature on the positron beam quality, the beams are propagated through the plasma column. In the simulations, both the drive and the witness beams are advanced with an adaptive time step, which resolves the betatron oscillation of the lower energy beam with 60 time steps per betatron period.

Results concerning the evolution of the projected emittance of the positron witness beam for plasma temperatures of 0 eV (blue line), 10 eV (green line), 50 eV (orange

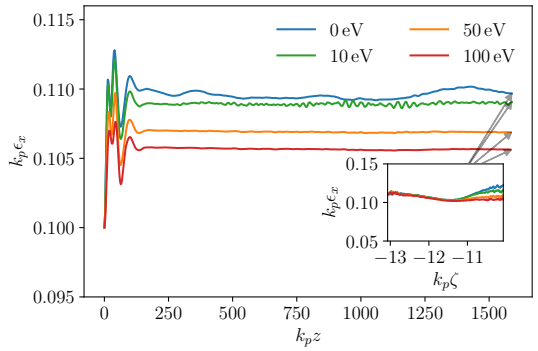

FIG. 5. Positron beam emittance as a function of the propagation distance for different temperatures. The emittance growth saturates at lower values for higher temperatures. The inset shows the final slice emittance along the bunch. Temperature effects mitigate the growth of the slice emittance at the head of the bunch. This agrees with the observation that temperature has a stronger effect on the transverse wakefield towards the head of the bunch, as shown in Fig. 3 (a).

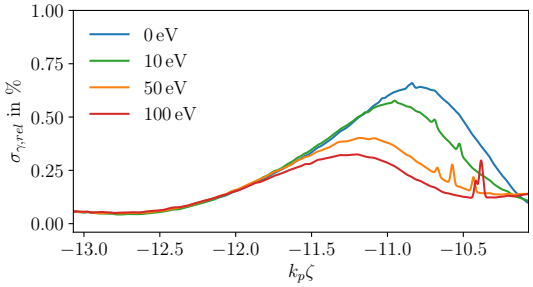

FIG. 6. Final relative slice energy spread of the positron bunch. The temperature reduces the slice energy spread more prominently at the head of the bunch, which is in agreement with the more flattened accelerating field at the head shown in Fig. 3 (b).

line), and 100 eV (red line) are shown in Fig. 5. In all cases, the emittance grows initially and then saturates. The emittance growth saturates at lower values for increasing temperatures. While the emittance increases for a plasma with a temperature of 0 eV by $\approx 10\,\%$, it only grows by 9 %, 7 %, and 6 % for a plasma temperature of 10 eV, 50 eV, and 100 eV, respectively. Thus, a temperature of tens to a hundred eV significantly reduces the emittance growth at saturation. To better understand the origin of the emittance decrease, the final slice emittances along the co-moving variable ζ are shown in the inset of Fig. 5. The biggest difference in the emittance is observed at the head of the bunch, while the emittance at the tail is minimally affected by the increasing temperature. The decrease in slice emittance at the head and unaffected slice emittance at the tail of the beam for increasing temperatures is consistent with the effect of the temperature on the transverse wakefields shown in Fig. 4 (a). Although it is possible to reduce the emittance growth in the cold plasma with slice-by-slice matching[8,33], the reduced slice-by-slice variation of the transverse wakefield due to the temperature improves the matching even for a longitudinally uniform beam profile.

The effect of the temperature on the slice energy spread is shown in Fig. 6. The final slice energy spread is significantly reduced for a warm plasma in the front part of the beam, which is in agreement with the transversely flattened longitudinal wakefield at the head of the beam shown in Fig. 4 (b). The overall energy spread is not much affected by a temperature in this setup, as the total energy spread is dominated by the longitudinal variation of the accelerating field due to imperfect beam-loading. However, in the case of an optimally loaded wake, the total energy spread is dominated by the slice energy spread[8] and thus, a temperature can help maintaining high beam quality.

In conclusion, temperature effects play a crucial role in positron acceleration in a plasma column: they significantly mitigate the emittance degradation and reduce the slice energy spread of an accelerated positron bunch in a plasma column by smoothing the wakefields transversely.

B. Positron acceleration in a hollow core plasma channel in the nonlinear regime

Hollow core plasma channels have been a promising candidate for high-quality positron acceleration[19,34,35], but they suffer from intrinsic instability due to the absence of focusing fields for symmetric particle beams[34,36]. A stable regime can be reached by using asymmetric drive beams[15]. Then, the asymmetric beam excites a quadrupole transverse wakefield within the hollow channel that determines the evolution of the asymmetric drive beam. As the beam is focused along its narrow transverse axis and defocused along its wider axis, it hits the channel wall in a controlled manner, providing stability. In the nonlinear regime, a sufficiently strong drive beam pushes the plasma electrons further into the channel wall. Then, the electrons are pulled back by the exposed ions, overshoot, and flow into the hollow plasma channel, forming an electron filament. By loading the filament with a positron bunch, more plasma electrons can be attracted, strengthening the filament. The scheme is illustrated in Fig. 7, where the normalized electron density is shown in the x-ζ-plane in (a). The ion background, the electron drive beam, and the positron witness beam are denoted in grey, red, and purple, respectively. The resulting transverse wakefield and a lineout of the on-axis longitudinal wakefield (black line) are shown in (b). As one can see, the on-axis electron filament between $-10 < k_p\zeta < -7$ generates both accelerating and focusing fields for positron beams.

In the original study the plasma was assumed to be cold. Here, we show by 3D PIC simulations that a temperature has a significant effect on the nonlinear wake structure within the electron filament, and that a tem-

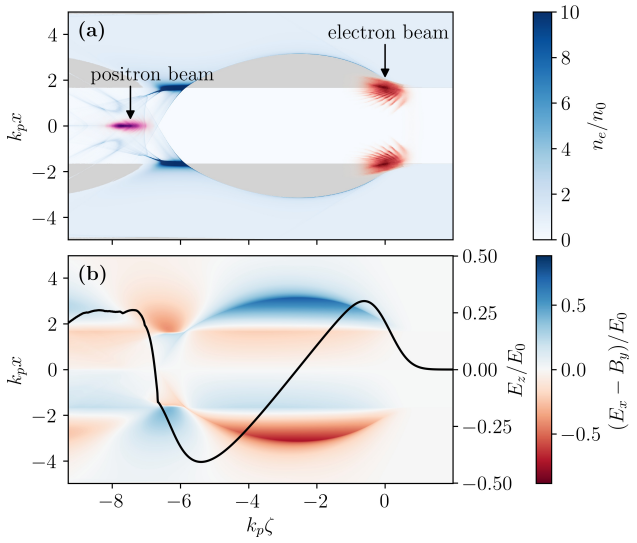

FIG. 7. Schematic of positron acceleration in a hollow core plasma channel. (a) Electron drive beam (red), positron witness beam (purple), normalized plasma density (blue), and ion background (grey) in the x-ζ-plane. The drive beam excites a plasma wake that pushes the plasma electrons into the channel wall. The electrons are pulled back by the ions such that the electrons flow into the hollow core channel and, supported by the attractive force of the positron witness bunch, generate a on-axis electron filament between $-10 < k_p\zeta < -7$. (b) Transverse wakefield in the x-ζ-plane (red-blue) and on-axis longitudinal wakefield (black line) along the co-moving variable ζ. The electron filament generates an accelerating and focusing field structure for positrons.

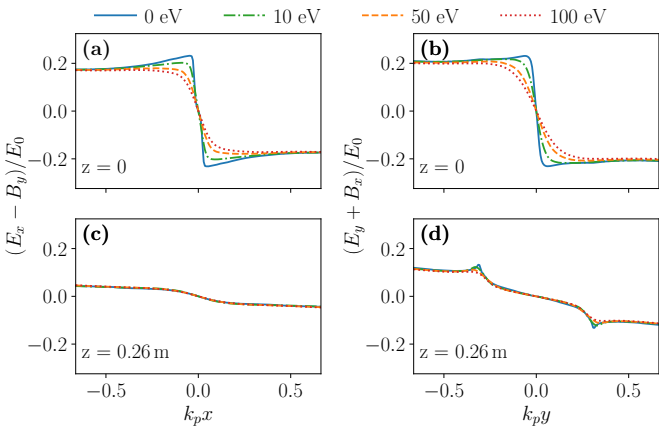

FIG. 8. Transverse wakefields $(E_x - By)/E_0$ [(a) and (c)] and $(E_y + B_x)/E_0$ [(b) and (d)] at the center of the positron witness beam at the plasma entrance [(a) and (b)] and at the plasma exit [(c) and (d)] for various plasma temperatures. The effect of the temperature is more pronounced at the beginning of the plasma, before the drive beam evolves to its equilibrium state.

perature mitigates the beam emittance degradation.

The effect is investigated by a similar setup to the one in the original study. The electron drive beam is of Gaussian shape with rms sizes $\sigma_{x,d} = 0.66\,k_p^{-1}$, $\sigma_{y,d} = 0.33\,k_p^{-1}$, and $\sigma_{\zeta,d} = 0.5\,k_p^{-1}$, a peak density of $n_d/n_0 = 6.5$, an energy of 5.11 GeV, and an emittance of $\epsilon_{x,d} = 0.66\,k_p^{-1}$ and $\epsilon_{y,d} = 0.44\,k_p^{-1}$. The positron witness beam is also a Gaussian beam with $\sigma_{x,w} = 0.17\,k_p^{-1}$, $\sigma_{y,w} = 0.13\,k_p^{-1}$, and $\sigma_{\zeta,w} = 0.5\,k_p^{-1}$, a peak density of $n_w/n_0 = 25.4$, an energy of 10.2 GeV, and an emittance of $\epsilon_{x,w} = 2.0\,k_p^{-1}$ and $\epsilon_{y,w} = 1.7\,k_p^{-1}$. The witness beam is located $7.5\,k_p^{-1}$ behind the drive beam. The drive and witness beam are modelled with 50×10^6 and 75×10^6 macro-particles, respectively. The beams are advanced with an adaptive time step using 60 time steps per betatron period.

The hollow core plasma has a background density of $n_0 = 3.11 \times 10^{16}\,\mathrm{cm}^{-3}$, an inner and outer radius of $1.7\,k_p^{-1}$ and $5\,k_p^{-1}$, respectively, and is modelled by 100 macro-particles per cell. In the simulations, the computational domain is $(-6.6, 6.6) \times (-6.6, 6.6) \times (-10, 4.5)\,k_p^{-3}$ in $x \times y \times \zeta$. The mesh resolution is $0.006 \times 0.006 \times 0.008\,k_p^{-3}$.

First, we investigate the influence of a temperature on the structure of the focusing field within the electron filament before evaluating its impact on the witness beam emittance. The wake changes significantly along the propagation in the plasma due to the evolution of the drive bunch, which must first reach its equilibrium state in the channel wall. Furthermore, due to the asymmetry of both the drive and the witness bunch, the transverse wakefield is also asymmetric in x and y. The initial (top plots) and the final (bottom plots) transverse wakefields are shown at the center of the witness bunch for a cold plasma (solid blue line), a plasma with 10 eV (dash-dotted green line), 50 eV (dashed orange line), and 100 eV (dotted red line) in Fig. 8. The initial transverse wakefields are highly non-linear and similar to the field structure observed in the plasma column. Again, the temperature leads to a significant smoothing of the non-linear part of the field. In the final state, the transverse wakefield in x exhibits close-to-linear behavior. The field is already a smooth function and the temperature does not show a visible effect. On the contrary, the final transverse wakefield in y has two non-linear bumps at $\approx \pm 0.33\,k_p^{-1}$, which are smoothed by temperature effects.

The smoothing of the non-linearity of the transverse wakefields due to the temperature affects the emittance evolution of the witness beam. The evolution of the emittance in the central slice of the bunch is shown in Fig. 9. The emittance grows in x (solid lines), and y (dashed lines) by $\approx$ 26 % and $\approx$ 18 %, respectively, in a cold plasma (blue lines). In a plasma with a temperature of 10 eV (green lines) the emittance grows in x (y) by 23 % (19 %). For a temperature of 50 eV (orange lines) the emittance growth in x (y) is 20 % (14 %). Finally, for a temperature of 100 eV (red lines) the emittance growth in x (y) is 16 % (11 %). Thus, in the given setup, a temperature of 50 eV and 100 eV can mitigate the emittance growth in both dimensions by roughly 20 % and 36 %,

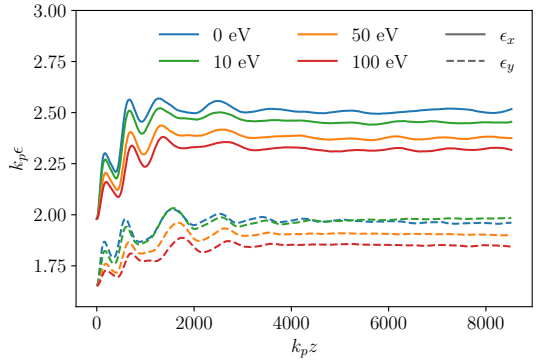

FIG. 9. Emittance of the central beam slice in x (solid lines) and y (dashed lines) along the propagation distance for different temperatures. The emittance growth saturates at lower values for higher temperatures.

respectively. Similar to the plasma column scheme, the slice energy spread is also affected by the temperature. In the hollow core scheme, the final central slice energy spread is 0.31 % in a cold plasma. This is reduced by 3 %, 6 %, and 11 % for a plasma with a temperature of 10 eV, 50 eV, and 100 eV.

Thus, the plasma electron temperature also has an significant effect on positron acceleration in a hollow core plasma accelerator using an asymmetric mode. It mitigates both emittance growth and slice energy spread at the central slice of the bunch.

IV. CONCLUSION

Temperature effects play an important role in both the modeling and the physics of plasma-based positron acceleration schemes that rely on high-density electron filaments. While a modest temperature of tens of eV does not affect, in general, electron acceleration in the blowout regime, in the case of positron acceleration it broadens the high-density electron filament used to generate the accelerating and focusing fields. The broadening of the electron filament has significant effects. In fact, the non-linearities of the transverse wakefields in the two different positron acceleration schemes analyzed are smoothed, leading to a significant mitigation of the emittance degradation for quasi-matched positron bunches. Furthermore, the longitudinal wakefield is also smoothed transversely, reducing the slice energy spread obtained by the positron bunch in plasmas with a temperature. Thus, a plasma temperature helps in the challenging task of preserving the beam quality in plasma-based positron accelerators. In addition, as discussed in the Appendix, a non-zero temperature helps with numerical convergence of the wakefields in the electron filament. We expect the plasma temperature effect observed and analyzed in this work to be relevant in other positron acceleration schemes relying on electron filaments, such as utilizing the back of the blowout bubble[11,12]. From the presented results, we conclude that is is important to include temperature effects in all positron acceleration schemes based on high-density electron filaments.

ACKNOWLEDGMENTS

This work was supported by the Director, Office of Science, Office of High Energy Physics, of the U.S. Department of Energy, under Contract No. DE-AC02-05CH11231 and used the computational facilities at the National Energy Research Scientific Computing Center (NERSC). We gratefully acknowledge the Gauss Centre for Supercomputing e.V. (www.gauss-centre.eu) for funding this project by providing computing time through the John von Neumann Institute for Computing (NIC) on the GCS Supercomputer JUWELS at Jülich Supercomputing Centre (JSC). This research was supported in part through the Maxwell computational resources operated at Deutsches Elektronen-Synchrotron DESY, Hamburg, Germany. We acknowledge the Funding by the Helmholtz Matter and Technologies Accelerator Research and Development Program.

DATA AVAILABILITY STATEMENT

The input scripts for the HiPACE++ simulations are openly available online[37]. The data that support the findings of this study are available upon reasonable request from the corresponding author.

Appendix: Temperature-dependent convergence scan

It is well-known that the spike of the longitudinal wakefield at the back of the blowout converges slowly in PIC simulations[27,38]. The reason is that the charge density of the returning electrons is difficult to resolve at the zero crossing. While this has negligible effect on energy gain and energy spread for electron acceleration, since there is no space to accelerate any electrons in the sharp field spike at the back of the bubble, it is significant for many positron acceleration schemes. The returning electrons form the filament in a finite extent around the zero crossing that is used for positron acceleration. Thus, it is of utmost importance to resolve precisely the area that is difficult to converge, imposing significant computational demands to plasma-based positron acceleration schemes. Similar to the field spike at the back of the blowout[27], a temperature helps alleviate the convergence issue of the wakefields in the electron filaments, since the momentum spread of warm plasma broadens the area of the zero crossing of the electrons.

We demonstrate this effect for the electron filament generated in a plasma column. The plasma and drive beam parameters are the same as in Sec. III A. The wake

is unloaded, i.e., no witness beam is present. The longitudinal resolution is fixed at $\Delta_\zeta = 0.002\,k_p^{-1}$. A convergence scan is performed in the transverse directions by increasing the number of transverse grid points N_x $(= N_y)$ from 1024 to 8192, corresponding to transverse resolutions of Δ_x $(= \Delta_y)$ from $0.031\,k_p^{-1}$ to $0.004\,k_p^{-1}$, respectively. Throughout the convergence scan a fixed number of 49 plasma particles per cell is used. A high number of plasma particles per cell is needed to ensure convergence in the presence of a plasma temperature, as the temperature can otherwise induce numerical noise. The resulting on-axis longitudinal wakefield E_z/E_0 along ζ (top plots) and the transverse wakefield $(E_x - B_y)/E_0$ along x at $\zeta = -10.5\,k_p^{-1}$ (bottom plots) are shown in Fig. 10 for various temperatures. The wakefields do not converge for a cold plasma (left column plots). As one can see, both wakefields at highest resolution (using 8192 grid points, dotted red lines) differ from the next lower resolution (4096 grid points, dashed green lines). When using 2048 grid points (dash-dotted orange lines) and 1024 grid points (solid blue lines) especially the transverse wakefield differs significantly from the highest resolution in the area around the zero-crossing at $x = 0$. Already at a temperature of 10 eV (center column plots) both the longitudinal and transverse wakefields agree reasonably well at the two highest resolutions. At a temperature of 50 eV (right column plots) neither the longitudinal nor the transverse wakefield shows significant difference between the two highest resolutions. At 50 eV, even the wakefields at a medium resolution of 2048 grid points are close to the converged fields at higher resolutions.

As anticipated from the spike at the back of the blowout, the fields in the electron filaments converge slowly for a cold plasma. Since this particular phase of the wakefields is crucial for positron acceleration, achieving high convergence is essential. Introducing temperature helps reduce the numerical requirements and enables convergence. Hence, a high resolution is still required for accurate results. Our findings suggest that the fields in previous studies of positron acceleration methods using cold plasmas[7,10,11,15] may not be fully converged, making it challenging to reproduce the results accurately, given their dependence on numerical subtleties, such as the number of iterations in the field solver. Therefore, future studies should include temperature effects when investigating positron acceleration in electron filaments.

[1] M. Litos, E. Adli, W. An, C. I. Clarke, C. E. Clayton, S. Corde, J. P. Delahaye, R. J. England, A. S. Fisher, J. Frederico, S. Gessner, S. Z. Green, M. J. Hogan, C. Joshi, W. Lu, K. A. Marsh, W. B. Mori, P. Muggli, N. Vafaei-Najafabadi, D. Walz, G. White, Z. Wu, V. Yakimenko, and G. Yocky, "High-efficiency acceleration of an electron beam in a plasma wakefield accelerator," Nature **515**, 92–95 (2014).

[2] C. A. Lindstrøm, J. M. Garland, S. Schröder, L. Boulton, G. Boyle, J. Chappell, R. D'Arcy, P. Gonzalez, A. Knetsch, V. Libov, G. Loisch, A. Martinez de la Ossa, P. Niknejadi, K. Põder, L. Schaper, B. Schmidt, B. Sheeran, S. Wesch, J. Wood, and J. Osterhoff, "Energy-spread preservation and high efficiency in a plasma-wakefield accelerator," Phys. Rev. Lett. **126**, 014801 (2021).

[3] S. Lee, T. Katsouleas, R. Hemker, E. Dodd, and W. Mori, "Plasma-wakefield acceleration of a positron beam," Phys. Rev. E **64**, 045501 (2001).

[4] M. J. Hogan, C. E. Clayton, C. Huang, P. Muggli, S. Wang, B. E. Blue, D. Walz, K. A. Marsh, C. L. O'Connell, S. Lee, R. Iverson, F.-J. Decker, P. Raimondi, W. B. Mori, T. C. Katsouleas, C. Joshi, and R. H. Siemann, "Ultrarelativistic-positron-beam transport through meter-scale plasmas," Phys. Rev. Lett. **90**, 205002 (2003).

[5] P. Muggli, B. E. Blue, C. E. Clayton, F. J. Decker, M. J. Hogan, C. Huang, C. Joshi, T. C. Katsouleas, W. Lu, W. B. Mori, C. L. O'Connell, R. H. Siemann, D. Walz, and M. Zhou, "Halo formation and emittance growth of positron beams in plasmas," Phys. Rev. Lett. **101**, 055001 (2008).

[6] S. Corde, E. Adli, J. Allen, W. An, C. Clarke, C. Clayton, J. Delahaye, J. Frederico, S. Gessner, S. Green, *et al.*, "Multi-gigaelectronvolt acceleration of positrons in a self-loaded plasma wakefield," Nature **524**, 442 (2015).

[7] S. Diederichs, T. J. Mehrling, C. Benedetti, C. B. Schroeder, A. Knetsch, E. Esarey, and J. Osterhoff, "Positron transport and acceleration in beam-driven plasma wakefield accelerators using plasma columns," Phys. Rev. Accel. Beams **22**, 081301 (2019).

[8] S. Diederichs, C. Benedetti, E. Esarey, J. Osterhoff, and C. B. Schroeder, "High-quality positron acceleration in beam-driven plasma accelerators," Phys. Rev. Accel. Beams **23**, 121301 (2020).

[9] S. Diederichs, C. Benedetti, M. Thévenet, E. Esarey, J. Osterhoff, and C. B. Schroeder, "Self-stabilizing positron acceleration in a plasma column," Phys. Rev. Accel. Beams **25**, 091304 (2022).

[10] K. V. Lotov, "Acceleration of positrons by electron beam-driven wakefields in a plasma," Physics of Plasmas **14**, 023101 (2007).

[11] S. Zhou, W. An, S. Ding, J. Hua, W. B. Mori, C. Joshi, and W. Lu, "Positron beam loading and acceleration in the blowout regime of plasma wakefield accelerator," (2022).

[12] W.-Y. Liu, X.-L. Zhu, M. Chen, S.-M. Weng, F. He, Z.-M. Sheng, and J. Zhang, "Tail-wave-assisted positron acceleration in nonlinear laser plasma wakefields," (2022).

[13] T. Wang, V. Khudik, and G. Shvets, "Positron acceleration in an elongated bubble regime," (2021).

[14] T. Silva, L. D. Amorim, M. C. Downer, M. J. Hogan, V. Yakimenko, R. Zgadzaj, and J. Vieira, "Stable positron acceleration in thin, warm, hollow plasma channels," Phys. Rev. Lett. **127**, 104801 (2021).

[15] S. Zhou, J. Hua, W. An, W. B. Mori, C. Joshi, J. Gao, and W. Lu, "High efficiency uniform wakefield acceleration of a positron beam using stable asymmetric mode in a hollow channel plasma," Phys. Rev. Lett. **127**, 174801 (2021).

[16] S. Green, E. Adli, C. Clarke, S. Corde, S. Edstrom, A. Fisher, J. Frederico, J. Frisch, S. Gessner, S. Gilevich, *et al.*, "Laser ionized preformed plasma at FACET," Plasma Physics and Controlled Fusion **56**, 084011 (2014).

[17] R. J. Shalloo, C. Arran, L. Corner, J. Holloway, J. Jonnerby, R. Walczak, H. Milchberg, and S. Hooker, "Hydrodynamic optical-field-ionized plasma channels," Physical Review E **97**, 053203 (2018).

[18] A. Picksley, A. Alejo, R. J. Shalloo, C. Arran, A. von Boetticher, L. Corner, J. A. Holloway, J. Jonnerby, O. Jakobsson, C. Thornton, R. Walczak, and S. M. Hooker, "Meter-scale conditioned hydrodynamic optical-field-ionized plasma channels," Phys. Rev. E **102**, 053201 (2020).

[19] S. Gessner, E. Adli, J. M. Allen, W. An, C. I. Clarke, C. E. Clayton, S. Corde, J. Delahaye, J. Frederico, S. Z. Green, *et al.*, "Demonstration of a positron beam-driven hollow channel plasma wakefield accelerator," Nature communications **7**, 11785 (2016).

[20] Y. Ehrlich, C. Cohen, A. Zigler, J. Krall, P. Sprangle, and E. Esarey, "Guiding of high intensity laser pulses in straight and curved plasma channel experiments," Physical review letters **77**, 4186 (1996).

[21] N. Bobrova, A. Esaulov, J.-I. Sakai, P. Sasorov, D. Spence,

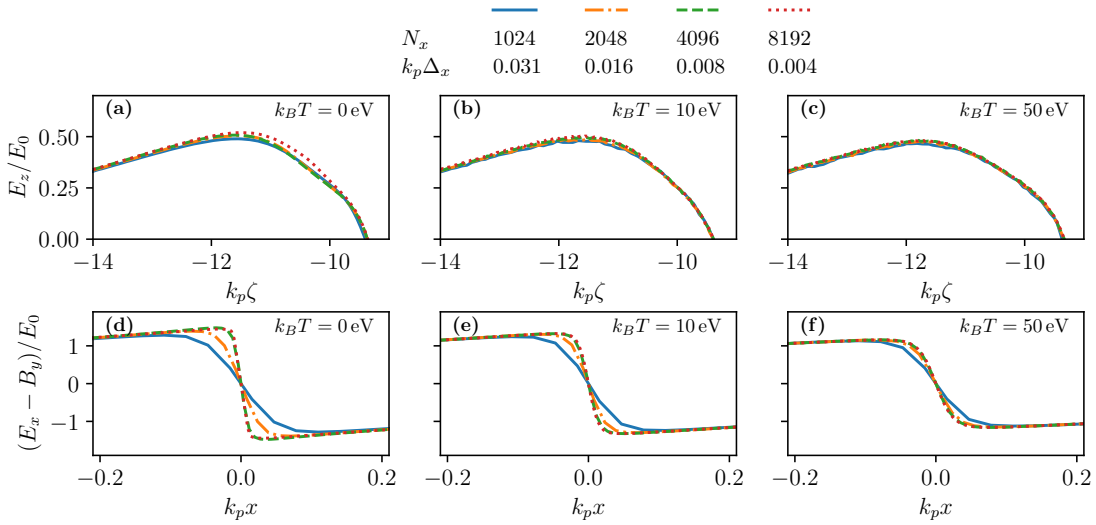

FIG. 10. Resulting wakefields for different transverse resolutions $k_p\Delta_x$, where N_x denotes the number of longitudinal grid points. On-axis longitudinal wakefield E_z for (a) a cold plasma, (b) a plasma at 10 eV, and (c) a plasma at 50 eV. Lineout of transverse wakefield E_z along transverse coordinate x at the longitudinal position of $k_p\zeta \approx -10.5$ for (d) a cold plasma, (e) a plasma at 10 eV, and (f) a plasma at 50 eV. At a cold plasma, convergence cannot be reached even for highest resolutions, while the fields converge at a reasonable temperature quite quickly.

A. Butler, S. M. Hooker, and S. Bulanov, "Simulations of a hydrogen-filled capillary discharge waveguide," Physical Review E **65**, 016407 (2001).

[22]T. Katsouleas and W. B. Mori, "Wave-breaking amplitude of relativistic oscillations in a thermal plasma," Phys. Rev. Lett. **61**, 90–93 (1988).

[23]J. B. Rosenzweig, "Trapping, thermal effects, and wave breaking in the nonlinear plasma wake-field accelerator," Phys. Rev. A **38**, 3634–3642 (1988).

[24]C. B. Schroeder, E. Esarey, and B. A. Shadwick, "Warm wave breaking of nonlinear plasma waves with arbitrary phase velocities," Phys. Rev. E **72**, 055401 (2005).

[25]C. B. Schroeder and E. Esarey, "Relativistic warm plasma theory of nonlinear laser-driven electron plasma waves," Phys. Rev. E **81**, 056403 (2010).

[26]K. V. Lotov, "Fine wakefield structure in the blowout regime of plasma wakefield accelerators," Phys. Rev. ST Accel. Beams **6**, 061301 (2003).

[27]N. Jain, J. Palastro, T. M. Antonsen, W. B. Mori, and W. An, "Plasma wakefield acceleration studies using the quasi-static code wake," Physics of Plasmas **22**, 023103 (2015).

[28]P. Mora and J. T. M. Antonsen, "Kinetic modeling of intense, short laser pulses propagating in tenuous plasmas," Physics of Plasmas **4**, 217–229 (1997).

[29]S. Diederichs, C. Benedetti, A. Huebl, R. Lehe, A. Myers, A. Sinn, J.-L. Vay, W. Zhang, and M. Thévenet, "HiPACE++: A portable, 3D quasi-static particle-in-cell code," Computer Physics Communications **278**, 108421 (2022).

[30]P. Mora and T. M. Antonsen, "Electron cavitation and acceleration in the wake of an ultraintense, self-focused laser pulse," Phys. Rev. E **53**, R2068–R2071 (1996).

[31]J.-L. Vay, A. Huebl, A. Almgren, L. D. Amorim, J. Bell, L. Fedeli, L. Ge, K. Gott, D. P. Grote, M. Hogan, R. Jambunathan, R. Lehe, A. Myers, C. Ng, M. Rowan, O. Shapoval, M. Thévenet, H. Vincenti, E. Yang, N. Zaïm, W. Zhang, Y. Zhao, and E. Zoni, "Modeling of a chain of three plasma accelerator stages with the WarpX electromagnetic PIC code on GPUs," Physics of Plasmas **28**, 023105 (2021).

[32]S. Diederichs, C. Benedetti, E. Esarey, M. Thévenet, J. Osterhoff, and C. B. Schroeder, "Stable electron beam propagation in a plasma column," Physics of Plasmas **29**, 043101 (2022).

[33]C. Benedetti, C. B. Schroeder, C. G. R. Geddes, E. Esarey, and W. P. Leemans, "Efficient modeling of laser-plasma accelerator staging experiments using inf&rno," AIP Conference Proceedings **1812**, 050005 (2017), https://aip.scitation.org/doi/pdf/10.1063/1.4975866.

[34]C. B. Schroeder, D. H. Whittum, and J. S. Wurtele, "Multimode analysis of the hollow plasma channel wakefield accelerator," Phys. Rev. Lett. **82**, 1177–1180 (1999).

[35]S. Zhou, J. Hua, W. Lu, W. An, Q. Su, W. B. Mori, and C. Joshi, "High efficiency uniform positron beam loading in a hollow channel plasma wakefield accelerator," Phys. Rev. Accel. Beams **25**, 091303 (2022).

[36]C. A. Lindstrøm, E. Adli, J. M. Allen, W. An, C. Beekman, C. I. Clarke, C. E. Clayton, S. Corde, A. Doche, J. Frederico, S. J. Gessner, S. Z. Green, M. J. Hogan, C. Joshi, M. Litos, W. Lu, K. A. Marsh, W. B. Mori, B. D. O'Shea, N. Vafaei-Najafabadi, and V. Yakimenko, "Measurement of transverse wakefields induced by a misaligned positron bunch in a hollow channel plasma accelerator," Phys. Rev. Lett. **120**, 124802 (2018).

[37]S. Diederichs, C. Benedetti, E. Esarey, M. Thévenet, A. Sinn, J. Osterhoff, and C. B. Schroeder, "HiPACE++ input scripts for "Temperature effects in plasma-based positron acceleration schemes using electron filaments"," (2023).

[38]S. Lee, T. Katsouleas, R. Hemker, and W. B. Mori, "Simulations of a meter-long plasma wakefield accelerator," Phys. Rev. E **61**, 7014–7021 (2000).